Barrier buckets in the CERN SPS

T. Bohl, T. Linnecar, E. Shaposhnikova
CERN, Geneva, Switzerland

Abstract

The use of barrier buckets to modify the azimuthal distribution of a beam in a circular accelerator has been described and demonstrated in several machines. Barrier buckets could become interesting for future modes of operation in the CERN SPS. Up to now the specially designed RF cavities used for this purpose have been very wide-band, capable of producing a single sine-wave. The existing 200 MHz Travelling Wave cavities in the SPS are not as wide-band but nonetheless have rise-times that are small compared with the revolution period. The possibility of using these cavities to provide "thick" barriers has been studied theoretically and experimentally in the SPS.

1 INTRODUCTION

Barrier buckets, as proposed in [1], have been explored in different laboratories [2], [3]. One possible application is to inject and rapidly debunch a beam to reduce space charge effects, limiting the azimuthal distance that can be occupied by the beam by using two barriers. This allows subsequent injections into the empty part of the ring. As an extension, the barriers can later be moved to compress the unbunched beam into an even smaller part of the ring. These two ideas have already been demonstrated in practice [2]. Acceleration of unbunched beams using barrier buckets has also been suggested [4].

In the CERN SPS, possible applications arise with the future CERN Neutrinos to Gran Sasso project. One would be to maintain an azimuthal hole during slow extraction of part of the beam at high energy. Fast extraction of the remaining beam could then be made in a clean way, the kicker field rising during the hole. A further possibility, mentioned already, occurs with the very high intensity beams that must be injected into the SPS so that local density effects are important.

In the references cited above, the barrier bucket was created with a single RF sinusoid using very wideband cavities. This provides a barrier which can be as short as one RF wavelength. The 200 MHz accelerating cavities in the SPS, while not being very wideband, are nonetheless of higher bandwidth than normally found in accelerators and can react in times significantly less than the revolution period 23 μs. They are of the untuned Travelling Wave (TW) type, quality factor $\sim$ 200, the four cavities giving up to a total of 8 MV. We have explored the possibility of using these cavities to create barriers in the SPS [5].

2 EXPERIMENTAL RESULTS

The minimum length of the barrier that can be created by a TW cavity is defined by the filling time, $\sim$ 600 ns. With constant power applied to the cavity the voltage rises linearly from zero to its maximum value as the field advances along the structure. When the power is switched off the field decays linearly in a similar time. In practice, these times are increased by the power amplifier risetime and the shape is no longer exactly linear. In Fig. 1 one can see the minimum pulse length that can be formed by switching off the drive to the power amplifiers the moment the voltage is maximum. The pulse shown is the detected RF voltage seen by the beam. The beam signal, taken from a longitudinal electrostatic pick-up, gives the batch envelope. Note also that due to reflection from the cavity loads, there is some RF voltage present between the RF pulses, but this is less than 10% of the maximum voltage.

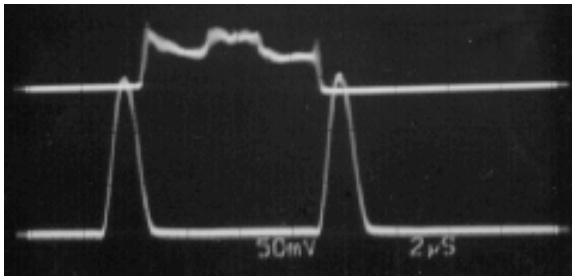

Figure 1: The beam current (top trace), held by two RF barriers (bottom trace).

The effectiveness of these barriers has been tested during machine development (MD) studies in the SPS below transition at 14 GeV/c, by injecting a 2 μs batch ($\sim$ 420 bunches) filling $\sim$ 1/11 of the circumference. Beam intensity for most experiments was $\sim 2 \times 10^{12}$ protons.

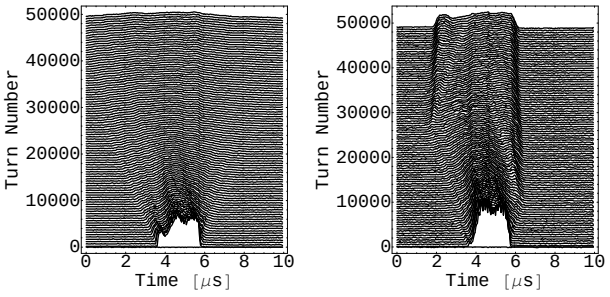

Figure 2: Mountain ranges: left, continuous debunching (RF off); right, beam held by barriers. 500 turns/trace.

With RF off, the beam debunches as shown in Fig. 2, left. When two RF pulses are applied, spaced by some time

greater than the beam length, the beam debunches as far as these pulses and is then reflected, see Fig. 2, right. In this example the RF pulses are not placed equally on either side of the beam - the beam hits the right barrier before the left.

It is important to adjust the RF frequency to a multiple of the revolution frequency of the central particles to center the barriers symmetrically in momentum. If this is not the case, the debunching becomes asymmetric and the beam moves towards one barrier where it is reflected and then moves towards the other barrier where it is again reflected. This situation is seen in Fig. 3, left.

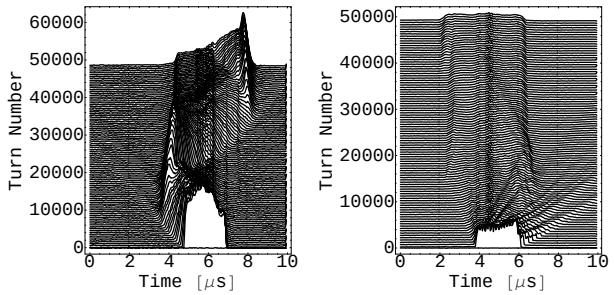

Figure 3: Mountain ranges: left, barriers at the shifted frequency; right, insufficient voltage. 500 turns/trace.

The initial voltage was 1 MV giving a bucket height, for the traditional RF system, of $\Delta p/p = \pm 2 \times 10^{-3}$, equal to the momentum spread in the injected beam. However, to hold the beam with barriers it was necessary to significantly increase the voltage, otherwise some particles could pass the barrier, see Fig. 3, right.

In our experiment it was also possible to allow the beam to debunch as far as barriers, placed about 6 μs away, and then to push the particles back again by moving the barriers closer together.

One other phenomenon that can be observed in Figs. 1-3, is the production of "ears" of density at the barriers - the reason is explained in the next section.

The situation at higher intensities was less easy to control. The debunching beam appears to become unstable with consequent increase in momentum spread. This has been observed before when high local intensity beams are debunched. It is probably due to the impedance of the TW cavities at frequencies near the edge of the accelerating pass-band. The maximum intensity that can be held is then limited by the maximum available voltage. Instabilities in single-period barrier bucket systems have been studied theoretically in [6].

3 ANALYSIS OF THE METHOD

The voltage applied to create the barrier buckets in the SPS can be presented in the general form:

$$V(\phi) = \begin{cases} V_0\, g(\phi)\, \sin(\phi + \phi_1), & \phi < 0, \\ V_0\, g(\phi)\, \sin(\phi + \phi_2), & \phi > 0, \end{cases} \qquad (1)$$

where ϕ_1 and ϕ_2 are constant phase shifts and $g(\phi)$ can be approximated by the following (see Fig. 1):

$$g(\phi) = \begin{cases} -(\phi + \phi_b)/\phi_p, & -(\phi_b + \phi_p) < \phi < -\phi_b \\ 0, & -\phi_b < \phi < \phi_b \\ (\phi - \phi_b)/\phi_p, & \phi_b < \phi < \phi_b + \phi_p \end{cases} \qquad (2)$$

where $2\phi_p$ is the total length of one RF pulse, and $2\phi_b$ is the batch length.

For these multi-period barrier buckets the potential well has the form

$$W(\phi) = \begin{cases} W_- = \frac{1}{\phi_p} \int_0^{\phi+\phi_b} \phi' \sin(\phi_b - \phi' - \phi_2) d\phi', \\ 0, \\ W_+ = \frac{1}{\phi_p} \int_0^{\phi-\phi_b} \phi' \sin(\phi_b + \phi' + \phi_1) d\phi', \end{cases} \qquad (3)$$

where the regions of applicability are as for $g(\phi)$ in (2).

As one can see, this potential well is symmetric, $W(-\phi) = W(\phi)$, only if $\phi_1 = -\phi_2$. Below, non-symmetric wells are not treated, so we assume $\phi_1 = -\phi_2 = \phi_0$.

In Fig. 4 the shape of the potential well around $\phi = 0$ is shown for $\phi_b = 0$, $\phi_0 = 0$ (left) and $\phi_0 = \pi$ (right). Independently of the shape of the potential wells around $\phi = 0$, barriers are provided earlier or later for particles moving between the two RF voltage pulses for any value of ϕ_0, different from the single-period barrier where phase is important. From now on we assume for simplicity that $\phi_0 = 0$.

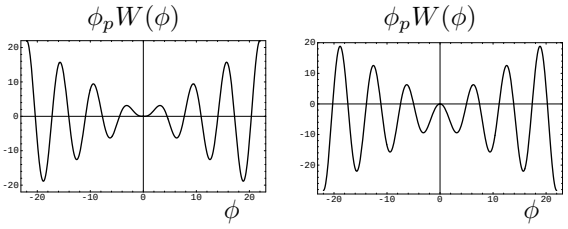

Figure 4: Potential well for $\phi_b = 0$, $\phi_0 = 0$ (left) and $\phi_0 = \pi$ (right).

For the experimental parameters in the SPS, which were $\phi_b \simeq 400\pi$ and $\phi_p \simeq 240\pi$, the potential well is shown in Fig. 5 (left). To see more detail we also present $\phi_b = 40\pi$ and $\phi_p = 24\pi$, Fig. 5 (right).

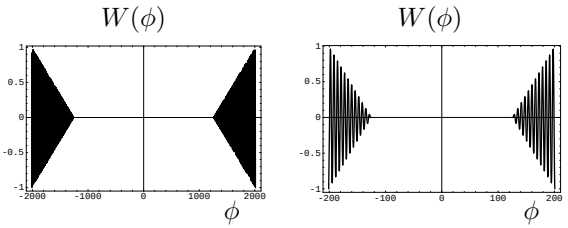

Figure 5: Potential well: SPS parameters (left); $\phi_b = 40\pi$, $\phi_p = 24\pi$ (right).

Unlike phase motion inside a standard RF buckets or between single-period barrier buckets, in our case the maximum energy deviation ΔE_{max} is reached by the particle

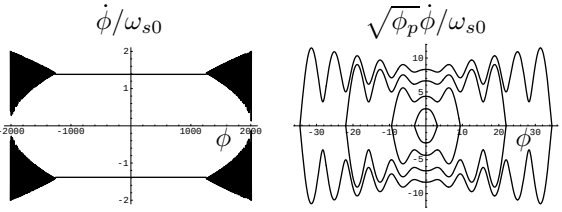

Figure 6: Limiting phase trajectory for SPS parameters (left), trajectories around $\phi = 0$ for $\phi_b = 0$ (right).

not at $\phi = 0$ (in the centre) but close to the maximum phase deviation ϕ_m, see phase trajectories in Fig. 6. The shape of the phase trajectories explain well the appearance of "ears" in the beam line density (see photo in Fig. 1 and mountain range displays in Fig. 2). For the motion between the barrier buckets, ΔE_{max} is related to the initial energy deviation of the particle ΔE_0 by

$$\Delta E_{max} \simeq \sqrt{2}\Delta E_0. \quad (4)$$

In a simple way this can be understood from the fact that the particle reflected by the wall at $\phi = \phi_m$ has an initial energy deviation ΔE_0 proportional to $\sqrt{W(\phi_m)}$ and its maximum energy deviation ΔE_{max} is proportional to $\sqrt{W(\phi_m) - W(\phi_{min})}$, where $W(\phi_{min})$ is the nearest minimum of $W(\phi)$. For multi-period barrier buckets $W(\phi_m) \simeq -W(\phi_{min})$ and therefore $\Delta E_{max} \simeq \sqrt{2}\Delta E_0$.

Note that normal RF buckets and barrier buckets (thin or thick) created by the same voltage amplitude V_0 have the same ΔE_{max}. However, a beam held by thick barrier buckets should have an initial energy spread $\sqrt{2}$ less to avoid particle loss. This explains why at the beginning of our experimental studies the voltage amplitude roughly estimated for a traditional RF system was insufficient to hold the beam with thick barrier buckets.

After capture, the final batch length is increased by the length of the RF pulse (depth of barrier) and becomes $2\phi_b + 2\phi_p$. The final longitudinal emittance ε is connected with initial ε_0 by the expression

$$\varepsilon \approx \varepsilon_0(1 + \frac{1+\sqrt{2}}{2}\frac{\phi_p}{\phi_b}). \quad (5)$$

In our experiments this gives approximately a factor 1.7 increase in the longitudinal emittance.

For problems of stability with a high intensity beam it is important to know the phase oscillation frequency distribution. For the potential well (3), the phase oscillation period can be found from expression

$$T_s(H) = \frac{2\sqrt{2}}{\omega_{s0}}\left[\frac{\phi_b}{\sqrt{H}} + \int_{\phi_b}^{\phi_b+\phi_p}\frac{d\phi}{\sqrt{H - W_+(\phi)}}\right], \quad (6)$$

where H is the Hamiltonian of the system and ω_{s0} is the synchrotron frequency in a traditional RF system with voltage amplitude V_0.

The phase oscillation frequency $\omega_s(H) = 2\pi/T_s(H)$ is presented in Fig. 7. The solid line on the top in Fig. 7 (left) shows the contribution from the first term in expression (6) which in fact describes the drift time in the region without field, $V = 0$. The resulting frequency is decreased by the time particles spend oscillating around the barrier buckets. The envelope of this frequency distribution is shown with dots in Fig. 7 (left). At every unstable fixed point the oscillation period becomes infinitely large and the corresponding phase oscillation frequency goes to zero. This creates a modulation of the phase oscillation frequency with the number of zeros equal to the number of RF periods in the pulse (~ 120 in our case) [1]. The fine structure of the frequency distribution for small H is presented in Fig. 7 (right).

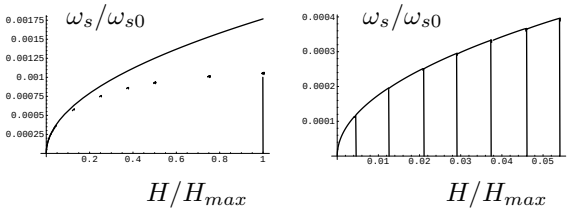

Figure 7: Left: phase oscillation frequency envelope (dots) plus contribution from drift (solid line) as a function of Hamiltonian H/H_{max}. Right: finer detail for small oscillation amplitudes.

4 CONCLUSIONS

Thick barrier buckets provided by the existing Travelling Wave RF system were able to hold a low-intensity proton beam. After capture the maximum energy spread in the system is larger by approximately a factor $\sqrt{2}$. The maximum energy spread is reached at the far ends of the beam. The increase in batch length is twice the cavity risetime.

Contrary to single-period, thin, barrier buckets, the choice of the RF phase (or voltage polarity) for thick barrier buckets is not critical for providing walls.

For thick barrier buckets the total frequency spread is smaller than (however comparable to) for thin barrier buckets. In both cases it is much smaller (by an order of magnitude) than in a traditional RF system. For thick barrier buckets the phase oscillation frequency has a fine structure leading to increased local frequency spread.

REFERENCES

[1] J.E. Griffin et al, IEEE Trans. Nucl. Sci. NS-30, p.3502, 1983.

[2] M. Blaskiewicz, J.M. Brennan, Proceed. EPAC96, p.2373, 1996.

[3] K.-Y. Ng, FERMILAB-FN-654.

[4] J. Kishiro, K. Takayama, KEK Preprint 98-210, 1998.

[5] T.Bohl, T.linnecar, E.Shaposhnikova, CERN SL-Note-2000-032 HRF, 2000.

[6] Y.H.Chin, H.Tsutsui, Proceed. PAC97, p.1545, 1997.

[1] This is true for a symmetric potential well. For a nonsymmetric potential well the number of zeros would be twice as large.